Influence of mung bean protein isolate concentration and pH on gel formation and physicochemical properties of mung bean protein–gellan gum composites

Praewa Lergchinnaboot[1], Nachomkamon Saengsuk[1,*], Chanikan Sonklin[2,3], Putthapong Phumsombat[1]

[1]School of Food Industry, King Mongkut's Institute of Technology Ladkrabang, Bangkok, Thailand; [2]Department of Industrial Chemistry, Faculty of Applied Science, King Mongkut's University of Technology North Bangkok, Wongsawang, Bangsue, Bangkok, Thailand; [3]Food and Agro-Industry Research Center, King Mongkut's University of Technology North Bangkok, Wongsawang, Bangsue, Bangkok, Thailand

*__Corresponding Author:__ Nachomkamon Saengsuk, School of Food Industry, King Mongkut's Institute of Technology Ladkrabang, 1 Chalong Krung 1 Alley, Lat Krabang, Bangkok 10520, Thailand. Email: nachomkamon.sa@kmitl.ac.th

Academic Editor: Slim Smaoui, PhD, Laboratory of Microbial, Enzymatic Biotechnology and Biomolecules (LBMEB), Center of Biotechnology of Sfax, University of Sfax-Tunisia, 3018 Sfax, Tunisia

Received: 3 February 2026; Accepted: 5 May 2026; Published: 10 June 2026

ORIGINAL ARTICLE

Abstract

This study examined the effects of mung bean protein isolate concentration and pH on gel formation and physicochemical properties of mung bean protein isolate–low-acyl gellan gum (MB-GG) composite systems for structured plant-based food applications. Composite gels were prepared using mung bean protein isolate concentrations of 25%, 50%, and 75% (w/w) under pH 5, 6, and 7 and evaluated for key physicochemical, structural, and rheological properties. Both mung bean protein isolate concentration and pH significantly influenced gel structure and functionality. Gels formed at pH 5 exhibited stronger intermolecular associations but more heterogeneous structures, potentially because of enhanced protein aggregation near the isoelectric region, whereas increasing pH improved gel uniformity and lightness while reducing water holding capacity. Although gels containing 25% mung bean protein isolate produced the strongest gel network, the 50% formulation at pH 6 provided the most balanced combination of structural stability, water retention, and textural performance. Overall, these findings demonstrate that balanced protein–gellan gum interactions, rather than protein enrichment alone, govern MB-GG gel functionality, and this interaction-driven framework may also guide formulation design in other plant protein–hydrocolloid systems for structured food applications.

Keywords: hydrocolloid; coacervation; alternative proteins; mung bean protein; gellan gum

Introduction

The global plant-based food industry has expanded rapidly in recent years, driven by increasing consumer awareness of environmental sustainability, health concerns, and animal welfare, compared to conventional meat-based foods. This shift in consumer preference has intensified the demand for plant-based meat alternatives that closely resemble animal meat in terms of taste, texture, aroma, and appearance. Among these attributes, texture is considered as one of the most critical factors influencing consumer acceptance of plant-based products (Ahmad *et al.*, 2022). Consequently, a major challenge in plant-based food development dwells in designing product structures that can effectively mimic the fibrous and elastic texture of meat, which requires the careful selection of protein sources, the incorporation of appropriate hydrocolloids, and precise control of processing conditions.

Mung bean (MB) residue, a by-product generated from mung bean (MB) processing, such as vermicelli or MB flour production, is typically underutilized and often treated as low-value waste. However, previous studies have reported that MB residue contains a considerable protein content, accounting for approximately 20–30% on a dry-weight basis, which can be recovered and valorized through protein extraction (Tang *et al.*, 2014). Recent studies have also highlighted the increasing interest in MB-based materials for their nutritional values and functional properties in food systems (Tripathi *et al.*, 2024). The production of protein isolates from MB residue therefore represents a promising approach for value addition, particularly from both economic and sustainability perspectives. Protein isolates derived from MB residue typically contain protein levels exceeding 80% (Badjona *et al.*, 2024) and exhibit functional properties suitable for plant-based meat applications, including gelation and three-dimensional (3D) network formation under controlled conditions, such as heating or pH adjustment. The functional performance of plant protein gels can be further enhanced by blending proteins with polysaccharides, which are known to improve structural integrity and water holding capacity (WHC). This strategy is particularly important in plant protein systems, where proteins alone often lack the structural stability and mechanical strength required for meat analogue applications. Among various polysaccharides, gellan gum (GG) has attracted considerable attention because of its excellent gel-forming ability. Gellan gum is a linear heteropolysaccharide belonging to the exopolysaccharide group and is produced by the bacterium *Sphingomonas paucimobilis* (Palumbo *et al.*, 2020). The importance of formulation balance in achieving desirable texture and structural stability has also been highlighted in structured plant-based food systems (Phumsombat *et al.*, 2024). In particular, low-acyl GG forms strong, transparent gels with high thermal stability, making it suitable for food applications that require a stable and well-defined structure (Kamer *et al.*, 2022).

Previous studies have shown that GG can interact with proteins through electrostatic interactions, hydrogen bonding, and phase separation mechanisms, leading to the formation of complex coacervates or composite gel networks. These interactions are strongly influenced by environmental conditions, such as pH, ionic strength, and concentrations of protein and polysaccharide, which govern charge distribution and molecular compatibility within the system. Consequently, GG has been widely applied to modify gel structure, improve mechanical properties, and enhance water retention in protein-based food systems. Several studies have demonstrated that GG can interact synergistically with plant proteins to strengthen gel networks, enhance WHC, and improve textural attributes, such as viscosity and elasticity (Liu *et al.*, 2022). Previous studies have also shown that such interactions are governed by electrostatic compatibility and phase behavior, which determine whether protein–polysaccharide systems form soluble complexes, coacervates, or composite gels. However, the final properties of protein–GG composite gels are highly dependent on the type of GG and the nature of protein–polysaccharide interactions. For instance, Li *et al.* (2025) reported that high-acyl GG formed strong and elastic gels when combined with potato protein, whereas low-acyl GG produced harder and more brittle gels under similar conditions. Similar formulation-dependent differences in gellan-mediated gel behavior and protein–polysaccharide interactions have been reported as well in other mixed biopolymer systems (Liu *et al.*, 2022; Palumbo *et al.*, 2020). The results indicate that gel behavior in protein–polysaccharide systems is strongly influenced by formulation parameters and environmental conditions, including MB protein isolate concentration and pH, which govern charge distribution and electrostatic interactions within the system. Although composite systems based on plant proteins and GG are widely investigated, no study has systematically examined the combined effects of pH and protein-to-polysaccharide ratio on gel formation in systems prepared from MB residue protein isolate and low-acyl GG. In particular, the combined effects of pH and MB protein isolate concentration on gel formation, structural organization, and physicochemical properties of such composite systems are not fully elucidated. It was hypothesized that pH and protein-to-polysaccharide ratio would significantly regulate the interactions between MB protein isolate and GG, thereby governing gel network formation, microstructure, and the resulting physicochemical and mechanical properties of the composite system. Therefore, the objective of this study was to determine how MB protein isolate concentration and pH influence gelation behavior, structural organization, and physicochemical properties of composite gels prepared with low-acyl GG. The findings of this work provide mechanistic insight into protein–polysaccharide gel network formation and practical guidance for the development of structured plant-based foods from underutilized agricultural by-products.

Materials and Methods

Materials

A MB protein isolate (protein 86.8%, moisture 6.9%, ash 3.9%) was purchased from Myskin Recipes (Chanjao Longevity Co., Ltd., Bangkok, Thailand). Low-acyl GG was obtained from Krungthepchemi (Bangkok, Thailand). All materials used in this study were of food-grade quality.

Optimization of mung bean protein isolate concentration and pH for gel formation

The sample preparation procedure is illustrated in Figure 1. This experiment was designed to determine the optimal MB protein isolate concentrations and pH conditions for gel formation in a MB protein isolate–GG system (MB-GG). The optimal conditions were determined following a dilute system approach, in which component interactions were first evaluated in simplified aqueous dispersions prior to thermal gelation, with minor modifications (Hu *et al.*, 2024). MB solution (10%, w/v) was prepared by dissolving MB protein isolate in deionized water and stirring overnight at 4°C. Separately, a GG solution (8%, w/v) was prepared by dissolving GG in deionized water overnight at 4°C. The reported proportions refer to the proportion of MB protein isolate in total biopolymer content (MB+GG) on a dry-weight basis. Both MB and GG solutions were mixed using MB protein isolate concentrations of 25%, 50%, and 75% (w/w), while the GG concentration was kept constant (25% w/w). The pH of each mixture was adjusted to values ranging from 5.0 to 7.0 using 0.1-M sodium hydroxide (NaOH) or 0.1-M hydrochloric acid (HCl), followed by stirring for 30 min. The mixtures were poured into 100-mL beakers (50 mm in diameter), which served as a mold, and then heated in a water bath at 85°C for 20 min, followed by continuous stirring for an additional 10 min. After heating, the samples were allowed to cool to room temperature and subsequently stored at 4°C for 24 h to induce gel formation. The optimal formulation conditions were selected based on the physical characterization described in the following sections.

Visual appearance and color

The visual appearance and color attributes of the protein–polysaccharide gels were evaluated to assess macroscopic quality differences among formulations. The visual appearance of gel samples was assessed through direct visual observation and photographic

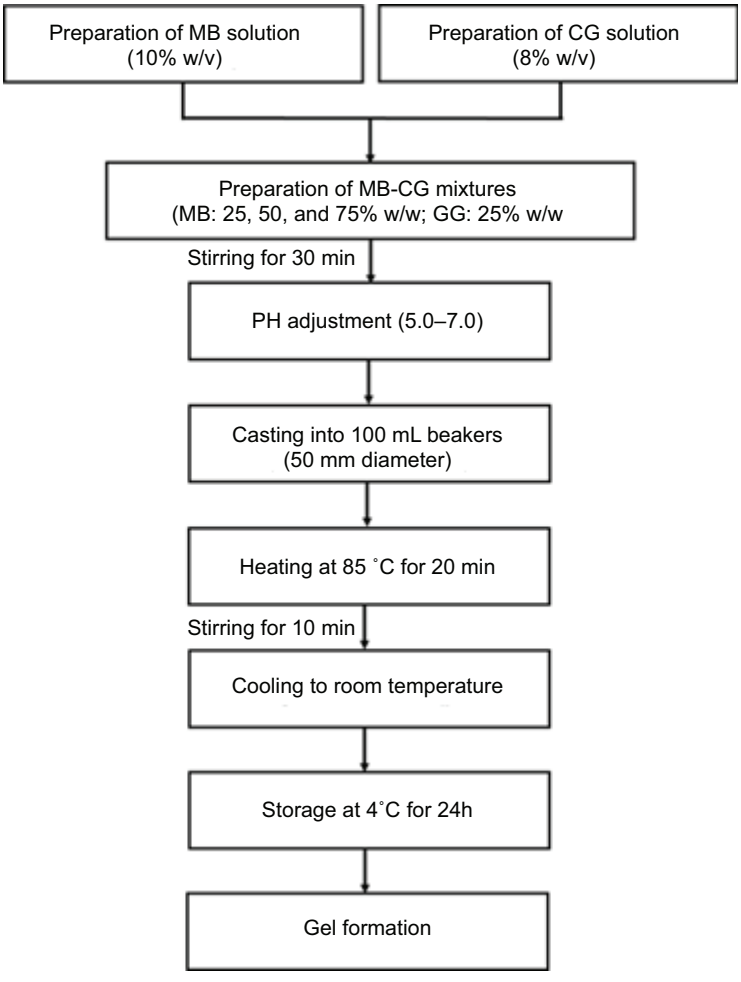

Figure 1. Flowchart of MB-GG gel formation optimization at different mung bean protein isolate concentrations and pH values.

documentation by following the method described by Ozorio *et al.* (2024). Color measurements were performed using a Hunter Lab colorimeter according to the procedure reported by Demircan *et al.* (2023). Color values were expressed in the International Commission on Illumination (CIE) Lab color space, where L* represents lightness (0 = black, 100 = white), a* indicates the green (–) to red (+) axis, and b* represents the blue (–) to yellow (+) axis.

Water holding capacity

Water holding capacity was measured as an indicator of gel network's ability to retain water after hydration by following a slightly modified method of Alavi *et al.* (2018). Solidified MB-GG gels (1–2 g) were mixed with 20 mL of distilled water and allowed to hydrate for 4 h at room temperature, with gentle stirring every 30 min to ensure uniform water absorption. After hydration, the samples were centrifuged at 3,000×g for 15 min. The supernatant was carefully decanted, and the wet weight of the gel was recorded immediately. The samples were then dried at 105°C until a constant weight was achieved, and the dry weight was recorded. WHC was calculated according to the following equation:

$$WHC\ (\%) = \frac{Wet\ weight - Dry\ weight}{Dry\ weight} \times 100, \quad \text{(Eqn. 1)}$$

WHC value represents the amount of water retained per gram of dry gel sample. This modified method was used to evaluate water retention after rehydration and centrifugal stress, thereby reflecting the practical water-binding stability of gel matrix.

Cooking loss

Cooking loss was determined based on weight changes before and after heating to reflect thermal stability of the gel structure. Each gel sample, prepared in a 100-mL beaker as a mold, was weighed before and after heating in a thermostatically controlled water bath (Memmert WNB14, Germany) at 85°C for 20 min, according to the method mentioned by Saengsuk *et al.* (2022). Cooking loss was expressed as the percentage difference between initial and final weights according to the following equation:

$$Cooking\ loss\ (\%) = \frac{Weight\ before\ cooking - Weight\ after\ cooking}{Weight\ before\ cooking} \times 100, \quad \text{(Eqn. 2)}$$

Texture profile analysis (TPA)

Textural properties of the gels were characterized using TPA under simulated mastication conditions. TPA was performed by compressing each sample twice to simulate human mastication by following the method described by Hu *et al.* (2024). The evaluated parameters included hardness, adhesiveness, springiness, cohesiveness, gumminess, and chewiness. Solidified MB-GG gels were cut into cubes of 1 × 1 × 1 cm prior to analysis. Texture measurements were carried out using a texture analyzer (TA-XT2, Stable Micro Systems, Surrey, UK) equipped with a cylindrical probe (P/50, 50 mm, stainless steel). The pre-test speed was set at 1 mm/s, while both test and post-test speeds were set at 5 mm/s. A strain of 75% was applied with a trigger force of 5 g, and the holding time at maximum compression was 5 s. The force–time curves were recorded by the instrument software, and textural parameters were calculated based on the obtained profiles.

Scanning electron microscopy (SEM)

The microstructural characteristics of the protein–polysaccharide gels were examined using SEM. MB-GG gel samples were cut into pieces of approximately 2 × 3 × 2 mm and fixed in 2.5% (v/v) glutaraldehyde prepared in 0.1-M sodium phosphate buffer (pH 7.2) for 2 h. The fixed samples were rinsed twice with the same buffer and once with distilled water, each for 15 min. Subsequently, the samples were dehydrated through a graded ethanol series (30–100%, v/v) for 10 min at each concentration. After dehydration, the samples were dried using a critical point dryer (EM CPD300, Leica Microsystems, Germany) and sputter-coated with gold for 2 min using a sputter coater (EM ACE200, Leica Microsystems, Germany). The microstructure of the samples was observed at a magnification of ×2,000 using a scanning electron microscope (Quanta 250, Czech Republic), which was selected to enable comparative observation of network morphology across formulations by following the method described by Saengsuk *et al.* (2021).

Rheological properties

Rheological analysis was performed using a Physica MCR 301 rheometer (Anton Paar, Graz, Austria) in oscillatory mode, fitted with a 50-mm parallel plate. The analysis was performed at a frequency of 1.0 Hz at 0.2% strain, within the linear viscoelastic region (pre-determined through frequency and amplitude testing) (Saengsuk *et al.*, 2023). A pH-adjusted mixture of MB-GG was heated between the parallel plates with a 1-mm gap. The

heating temperature ranged from 20°C to 80°C, and the cooling temperature ranged from 80°C to 20°C. The temperature was increased and decreased at a rate of 2°C/min using the rheometer temperature control system. Both energy storage modulus (G') and energy loss modulus (G") values were recorded.

Zeta potential

Zeta potential was measured to evaluate the electrostatic stability of the MB-GG dispersions and to characterize interactions among samples with different MB protein isolate concentrations and pH within the dispersion system. Dispersion samples were diluted 100-fold with deionized water and analyzed using a Nanoparticle Size Analyzer (SZ-100V2, HORIBA, Japan). Particle size and distribution were determined using dynamic light scattering (DLS), while zeta potential was measured using Laser Doppler Electrophoresis in plus mode, with a detection range of −500–+500 mV. All measurements were conducted in triplicate at room temperature.

Fourier transform infrared spectroscopy (FTIR)

Fourier transform infrared spectroscopy was employed to investigate molecular interactions and secondary structural changes in the protein–polysaccharide gels. Attenuated total reflectance–Fourier transform infrared (ATR-FTIR) spectra were recorded using a Spectrum 3 Tri-Range FTIR spectrometer (PerkinElmer, Austria). Lyophilized samples (5 mg) were placed directly onto the diamond ATR crystal. Spectra were collected over the range of 4,000–650 cm^{-1} with a resolution of 4 cm^{-1} and 32 scans per sample. The obtained spectra were processed and analyzed using the OriginLab software (Northampton, MA, USA). To evaluate changes in protein secondary structure, peak deconvolution of the amide I region (1,700–1,600 cm^{-1}) was performed using the second derivative method and Gaussian curve fitting by following the procedure described by Taheri *et al.* (2025).

Statistical analysis

All experimental measurements were conducted in triplicate, and the results were expressed as mean ± standard deviation (SD). Statistical analysis was performed using one-way analysis of variance (ANOVA), followed by Duncan's multiple range test, with the IBM SPSS Statistics software (version 29.0.1.1, IBM Corp., Armonk, NY, USA). Differences were considered statistically significant at $P < 0.05$.

Results and Discussion

Visual appearance of mung bean protein–gellan gum gels

The visual appearance of MB-GG gels prepared at different MB protein isolate concentrations and pH conditions is shown in Figure 2. Clear differences in gel appearance were observed as a function of both MB protein isolate concentration and pH. Gels prepared with 25% MB protein isolate exhibited a smooth, uniform surface and good structural integrity, particularly at pH 6 and 7. In contrast, gels formed at lower pH values or at higher MB protein isolate concentrations (50% and 75%) appeared less homogeneous, with rougher surfaces and reduced structural stability.

These observations indicate that both MB protein isolate concentration and pH play critical roles in determining the macroscopic quality of MB-GG gels. Formulations prepared under near-neutral pH conditions and at an intermediate MB protein isolate concentration favored the formation of visually uniform and stable gel structures, suggesting improved compatibility between MB protein isolate and GG under these conditions. This behavior can be explained by pH-dependent changes in protein surface charge relative to its isoelectric point. At lower pH conditions, MB protein carries a reduced net negative charge, which promotes electrostatic interactions with the negatively charged GG, leading to aggregation and less uniform structures. In contrast, at near-neutral pH, improved charge balance between the two components enhances molecular compatibility and facilitates the formation of more homogeneous and stable gel networks. This observation may also suggest that GG plays a dominant role in gel network formation, acting as a primary gelling agent within the system, while MB protein primarily contributes to modifying the network structure and mechanical properties.

Water holding capacity and cooking loss

Water holding capacity of MB-GG composites at different MB protein isolate concentrations and pH levels is summarized in Table 1. Significant differences in WHC were observed among formulations ($P < 0.05$), indicating that both MB protein isolate concentration and pH markedly influenced the water-binding properties of gels. For all formulations, the highest WHC values were obtained at pH 5, followed by a gradual decrease as pH increased to 6 and 7. At 25% MB protein isolate, WHC decreased from 26.45% at pH 5 to 19.85% at pH 7. A similar trend was observed at 50% MB protein isolate, which exhibited the highest WHC value among all formulations at pH 5 (27.89%). In contrast, gels prepared with 75% MB protein isolate showed significantly lower

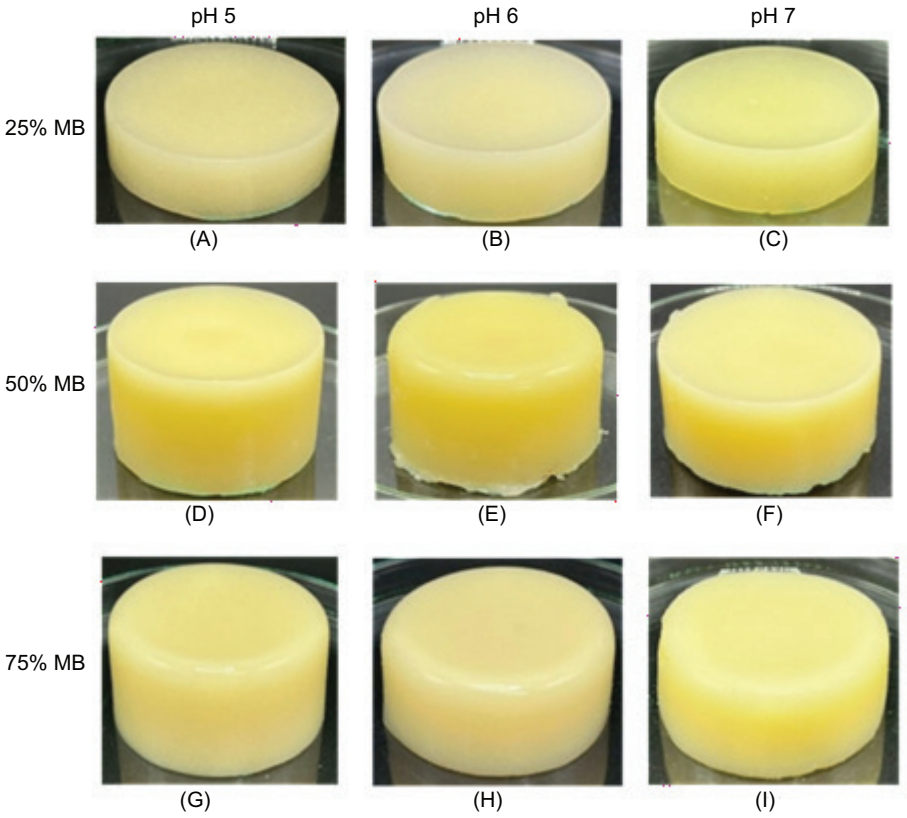

Figure 2. Appearance of MB-GG composites at different mung bean protein isolate concentrations and pH values.

Table 1. Water holding capacity and cooking loss of the mung bean protein isolate–low-acyl gellan gum (MB-GG) composite.

MB concentrations(% w/w)	pH	WHC (%)	Cooking loss (%)
25	5	26.45 ± 1.22^{a,b}	2.04 ± 0.30^{a}
	6	21.51 ± 1.55^{b,c}	1.62 ± 0.03$^{b–d}$
	7	19.85 ± 3.43^{c,d}	1.48 ± 0.04^{c,d}
50	5	27.89 ± 5.66^{a}	1.85 ± 0.16^{a,b}
	6	14.65 ± 5.22^{d,e}	1.68 ± 0.07^{b,c}
	7	12.84 ± 1.75^{e}	1.56 ± 0.06$^{b–d}$
75	5	20.50 ± 2.26^{c}	1.55 ± 0.18^{c,d}
	6	11.95 ± 1.01^{e}	1.36 ± 0.16^{d}
	7	9.94 ± 0.33^{e}	0.99 ± 0.17^{e}

Notes: Values are expressed as mean ± SD (n = 3).
Different superscript alphabets within the same column indicate significant differences among formulations according to Duncan's multiple range test ($P < 0.05$). MB: mung bean; WHC: water holding capacity.

WHC values at all pH levels, with the lowest WHC observed at pH 7 (9.94%). The markedly lower WHC observed at 75% MB protein isolate suggests a critical concentration, beyond which further addition of protein becomes detrimental. At high protein levels, excessive protein–protein interactions dominate, leading to a dense and aggregated network with reduced pore connectivity and fewer available sites for water binding. In

addition, the imbalance between protein and GG disrupts optimal composite network formation, limiting water entrapment. As a result, excess protein promotes water expulsion and reduces WHC.

When comparing different MB protein isolate concentrations at the same pH, the formulation containing 50% MB protein isolate generally exhibited higher WHC than that containing 25%, whereas the formulation containing 75% MB protein isolate consistently resulted in significantly lower WHC values ($P < 0.05$). These results demonstrate that both pH and MB protein isolate concentration play critical roles in determining the WHC of MB-GG gel systems.

The observed enhancement of WHC under weak acidic conditions (pH 5) can be attributed to improved protein–polysaccharide interactions and the formation of a more effective 3D network capable of immobilizing water. At pH 5, MB protein approaches its isoelectric region (approximately pH 4.5–5.0), resulting in reduced net charge and improved association with GG, which favors the formation of a more compact and water-retaining gel network (Tarahi *et al.*, 2024). Similar observations were reported by Ryu and McClements (2024), who showed that the incorporation of appropriate polysaccharides into plant protein systems promoted network development and significantly increased WHC. These results are also consistent with previous studies demonstrating that the incorporation of functional carbohydrates or hydrocolloids can significantly influence the structural and functional performance of protein-based systems (Namkieat *et al.*, 2025). Notably, the present results suggest that WHC was governed not only by total protein content but also by the balance between protein–polysaccharide association and network continuity. The superior WHC observed at intermediate protein content indicates that balanced interactions between MB protein and GG are more effective for water immobilization than protein enrichment alone.

Cooking loss values of MB-GG composites under different formulation conditions are also presented in Table 1. In contrast to WHC, cooking loss tended to decrease with increasing pH across all MB protein isolate concentrations. The lowest cooking loss was observed for gels prepared with 75% MB protein isolate at pH 7 (approximately 0.99%), while higher cooking losses were generally associated with lower pH conditions. These results indicate that cooking loss is strongly influenced by both MB protein isolate concentration and pH, reflecting differences in thermal stability and structural integrity of the gel network during heating.

Reduced cooking loss at higher pH values and higher MB protein isolate concentrations may be associated with structural rearrangements of the protein network and the formation of a more thermally stable gel matrix. Such structures are better able to retain water during heating, thereby reducing mass loss. Similar trends are reported in structured plant-based and meat analogue systems, where the incorporation of binders and hydrocolloids improved network stability and reduced cooking losses (Sha and Xiong, 2020; Sim *et al.*, 2025; Wi *et al.*, 2020). Importantly, the present results suggest that cooking loss is not solely governed by total water content but also by the ability of protein–polysaccharide networks to maintain structural integrity under thermal processing.

Color characteristics

The color characteristics of MB-GG composites prepared at different protein levels and pH conditions are presented in Table 2. Significant differences in L*, a*, and b* values were observed among formulations ($P < 0.05$), indicating that both protein level and pH markedly influenced the optical properties of gels. The lightness (L*) values generally increased with increasing MB protein isolate concentration from 25% to 75% across all pH levels. The highest L* values were observed at pH 7, particularly for gels prepared with higher MB protein isolate concentrations.

All samples exhibited negative a* values, indicating a greenish color tone. The magnitude of negative a* values increased with increasing pH, suggesting a more pronounced green hue under near-neutral pH conditions. This trend was especially evident for gels prepared with 75% MB protein isolate. In contrast, b* values generally increased with increasing MB protein isolate concentration, indicating enhanced yellowness, while a decreasing trend in b* values was observed as pH increased from 5 to 7.

The observed changes in color characteristics are attributed to variations in MB protein isolate concentration and protein–polysaccharide interactions within the gel matrix. Increased protein content potentially increased optical opacity through enhanced light scattering by dispersed protein-rich domains within the gel matrix. This effect is consistent with increased phase heterogeneity and reduced light transmission in protein-enriched systems, which contributed to higher L* values observed at elevated MB protein isolate concentrations. This phenomenon is primarily associated with microstructural light scattering rather than macroscopic phase separation, as no visible phase separation or structural discontinuity was observed in gel systems, although pH-induced changes in protein charge and structural

Table 2. Color characteristics of mung bean protein isolate–low-acyl gellan gum (MB-GG) composite.

MB concentrations (% w/w)	pH	Color values		
		L*	a*	b*
25	5	48.23 ± 2.96^{c}	–2.22 ± 0.09^{b}	4.08 ± 0.96^{c,d}
	6	47.65 ± 2.56^{c}	–2.84 ± 0.25^{c,d}	3.74 ± 0.64^{d}
	7	45.39 ± 2.01^{d}	–4.08 ± 0.22^{e}	2.15 ± 0.64^{e}
50	5	49.70 ± 1.07^{b,c}	–1.93 ± 0.08^{a}	4.74 ± 0.17^{b,c}
	6	51.44 ± 3.19^{a,b}	–2.70 ± 0.50^{c}	5.06 ± 1.52^{b}
	7	51.41 ± 2.25^{a,b}	–3.92 ± 0.21^{e}	3.79 ± 0.58^{d}
75	5	50.89 ± 1.58^{a,b}	–3.03 ± 0.06^{d}	6.88 ± 0.26^{a}
	6	51.01 ± 1.79^{a,b}	–4.06 ± 0.11^{e}	6.72 ± 0.80^{a}
	7	52.78 ± 0.74^{a}	–4.91 ± 0.07^{f}	5.52 ± 0.09^{b}

Notes: Values are expressed as mean ± SD (n = 3).
Different superscript alphabets within the same column indicate significant differences among formulations according to Duncan's multiple range test ($P < 0.05$). MB: mung bean.

organization potentially altered light scattering and chromatic response within the gel matrix. Similar effects of formulation and pH on color attributes are reported in plant-based protein systems by Demircan *et al.* (2023). These optical differences were consistent with the structural and functional trends observed in Sections 3.2 and 3.4, where formulations with greater opacity and yellowness also tended to exhibit lower WHC and weaker textural properties. This relationship suggests that color variation in MB-GG gels was not only a visual attribute but also an indirect indicator of internal network organization and water distribution. Overall, these results emphasize the importance of formulation design and pH control in achieving desirable color attributes for plant-based protein gel products.

Texture profile analysis

The results of TPA of MB-GG gels prepared under different formulation conditions are summarized in Table 3. Significant differences in textural parameters, such as hardness, adhesiveness, springiness, cohesiveness, gumminess, and chewiness, were observed as a function of both MB protein isolate concentration and pH ($P < 0.05$). Gel hardness was strongly affected by formulation, with the highest values consistently observed in gels containing 25% MB at pH 6 and 7. In contrast, gels prepared with higher protein levels (50% and 75% MB) exhibited significantly lower hardness across all pH conditions.

Similar formulation-dependent trends were observed for secondary textural parameters. In general, gels with higher hardness also showed greater gumminess and chewiness, confirming the formation of a stronger and more mechanically resistant gel matrix. By contrast, formulations with higher protein content exhibited lower overall textural strength, while variations in adhesiveness and springiness were less pronounced.

The enhanced hardness and mechanical strength observed at a 25% MB protein isolate, particularly at pH 6–7, may be attributed to favorable interactions between 25% MB protein isolate and GG near the protein's isoelectric region (approximately pH 4.5–5.0), facilitating the formation of a continuous and robust polysaccharide-dominated gel network (Dakhili *et al.*, 2026). Similar structure–function relationships between protein–hydrocolloid interactions and textural properties are reported in restructured protein systems (Phumsombat *et al.*, 2025; Sonklin *et al.*, 2026). In contrast, increasing protein content appears to disrupt network continuity, potentially because of intensified protein–polysaccharide interactions and complex coacervation that limit the availability of GG for forming effective network. This mechanism is governed by the charge characteristics of components. GG carries negatively charged carboxyl groups, whereas MB protein exhibits pH-dependent surface charge with an isoelectric point around pH 4.5–5.0. Near this region, reduced net charge on protein facilitates electrostatic interactions with GG, promoting associative phase separation. Comparable antagonistic effects of excess protein on gel strength in mixed protein–polysaccharide systems are reported as well (Babaei *et al.*, 2019; Salminen *et al.*, 2022). A comparable reduced hardness with increased protein loading is reported in

Table 3. Texture properties of the mung bean protein isolate–low-acyl gellan gum (MB-GG) composite.

MB (% w/w)	pH	Hardness (g)	Adhesiveness (g.s)	Springiness (mm)	Cohesiveness (ratio)	Gumminess (g)	Chewiness (g × mm)
25	5	927.06 ± 253.16^{b}	–6.87 ± 3.19^{a}	0.37 ± 0.09$^{a–c}$	0.11 ± 0.01^{d,e}	100.85 ± 39.11^{c}	37.62 ± 17.96^{b}
	6	1517.42 ± 341.37^{a}	–7.20 ± 4.73^{a}	0.41 ± 0.13^{a}	0.11 ± 0.02^{d}	175.56 ± 61.32^{b}	74.21 ± 41.17^{a}
	7	1523.38 ± 332.32^{a}	–6.64 ± 3.28^{a}	0.36 ± 0.07$^{a–c}$	0.14 ± 0.02^{c}	223.09 ± 73.85^{a}	79.71 ± 28.23^{a}
50	5	564.91 ± 158.03^{c}	–7.59 ± 3.77^{a}	0.31 ± 0.05^{b,c}	0.10 ± 0.01^{e}	56.05 ± 21.90^{e}	17.36 ± 7.34^{c}
	6	584.35 ± 196.60^{c}	–6.88 ± 4.76^{a}	0.40 ± 0.10^{a}	0.11 ± 0.01^{d}	68.00 ± 30.85^{d,e}	26.14 ± 9.27^{b,c}
	7	576.27 ± 78.19^{c}	–8.19 ± 4.36^{a,b}	0.38 ± 0.8^{a,b}	0.16 ± 0.01^{b}	94.68 ± 19.78^{c,d}	35.36 ± 8.55^{b}
75	5	441.33 ± 120.57^{c,d}	–6.08 ± 3.34^{a}	0.30 ± 0.11^{c}	0.11 ± 0.02^{d}	51.05 ± 21.62^{e}	15.27 ± 7.85^{c}
	6	466.98 ± 89.75^{c,d}	–10.65± 5.28^{b,c}	0.41 ± 0.10^{a}	0.14 ± 0.01^{c}	66.93± 18.18^{d,e}	27.23 ± 9.02^{b,c}
	7	407.51 ± 80.14^{d}	–11.87 ± 4.79^{c}	0.32 ± 0.07^{b,c}	0.22 ± 0.02^{a}	90.91 ± 22.08^{c,d}	29.77 ± 11.64^{b,c}

Notes: Values are expressed as mean ± SD (n = 5).
Different superscript alphabets within the same column indicate significant differences among formulations according to Duncan's multiple range test ($P < 0.05$). MB: mung bean.

plant protein–polysaccharide composite gels, where excessive addition of protein disrupted matrix continuity and reduced gel firmness by approximately 40–60% relative to balanced formulations (Salminen *et al.*, 2022). A similar magnitude of reduction was observed in the present study, where hardness decreased from approximately 1,520 g in the 25% MB system to 408–584 g in higher-protein formulations.

Microstructural characteristics

The microstructural features of MB-GG gels were further examined using SEM, as presented in Figure 3. SEM images revealed pronounced differences in network architecture among different formulations. Gels prepared with 25% MB protein isolate and pH 6–7 exhibited a dense, continuous, and well-connected network structure. The microstructure appeared more compact and homogeneous compared to other formulations, although pore size could not be clearly resolved at the applied magnification. It should be noted that SEM observations were used for qualitative comparison of network morphology, and precise pore size analysis was beyond the resolution of the current imaging conditions. Such microstructures are indicative of a more compact and structurally cohesive gel matrix.

In contrast, gels prepared at lower pH values or with higher MB protein isolate concentrations showed more heterogeneous microstructures characterized by less compact organization, disrupted network continuity, and reduced connectivity. These structural differences suggest weaker intermolecular associations and less effective network formation. At higher protein levels, excess MB protein probably promoted aggregation and phase crowding, which reduced the effective continuity of the GG-supported matrix and resulted in a more heterogeneous microstructure. The observed microstructural variations are consistent with protein–polysaccharide interactions governed by electrostatic effects, where favorable charge interactions at near-neutral pH and appropriate MB protein isolate concentrations promote complex coacervation and network development. Similar trends were reported by Ryu and McClements (2024), who demonstrated that complex coacervation significantly influences the microstructure and mechanical behavior of plant protein–polysaccharide gel systems. These results are consistent with previous studies on protein–polysaccharide coacervation systems, where the formation of compact and continuous network structures is reported to depend strongly on pH and component ratios. Similar structural behaviors are observed in canola protein and sesame protein systems interacting with polysaccharides, where optimal charge balance led to enhanced network formation and reduced porosity (Moghadam *et al.*, 2025).

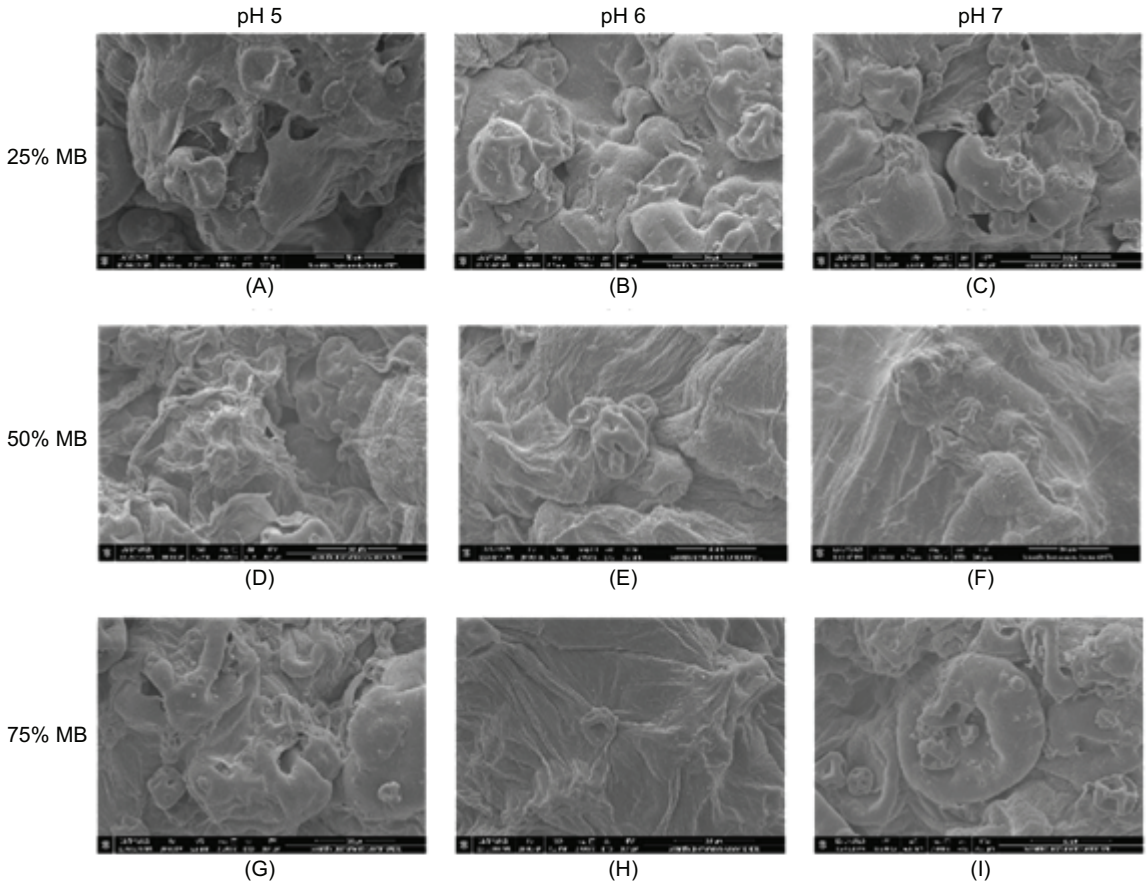

Figure 3. SEM micrographs of MB-GG composite gels prepared at different protein-to-gellan gum ratios (1:1, 2:1, and 3:1) and pH conditions (5, 6, and 7). Panels (A–C), (D–F), and (G–I) correspond to 1:1, 2:1, and 3:1 MB-GG ratios, respectively, while columns represent pH 5, 6, and 7 from left to right. All images were obtained at magnification ×2,000. Scale bars = 50 µm.

Rheological properties

The rheological behavior of MB-GG composites during heating and subsequent cooling is illustrated in Figure 4, and the corresponding G' and G'' values at key temperatures are summarized in Table 4. Across all formulations, both G' and G'' increased markedly during heating from 20°C to 80°C, indicating progressive development of a gel network upon thermal treatment. During the cooling phase, further increase in G' was observed, suggesting continued network reinforcement and stabilization (Chassenieux and Nicolai, 2024; Malkin and Derkach, 2024).

The magnitude of G' was consistently higher than that of G'' throughout the heating and cooling cycles for all formulations, confirming the formation of elastic-dominant gel systems (Malkin *et al.*, 2023). Notably, gels prepared with 25% MB protein isolate exhibited the highest G' values after heating and cooling, particularly at pH 5 and 6. As shown in Table 4, the G' value of the formulation containing 25% MB protein isolate at pH 5 increased from 6,080 Pa at 20°C to 215,000 Pa after heating, and further increased to 406,000 Pa after cooling to 20°C, indicating the formation of a strong and stable gel network.

In contrast, formulations with higher protein-to-GG ratios generally exhibited weaker or less stable viscoelastic behavior despite showing a similar temperature-dependent gelation trend. For example, at pH 5, the G'value of the formulation containing 75% MB protein isolate increased to 139,500 Pa after heating and 568,000 Pa after cooling; however, the corresponding G'' values also increased substantially, reflecting a comparatively weaker and more dissipative network structure. Although the 75% MB formulation exhibited a higher final G' after cooling under this condition, the concurrent increase in G'' indicates that the resulting structure was more dissipative and less mechanically stable, suggesting that elevated modulus alone did not reflect superior gel network quality. These results

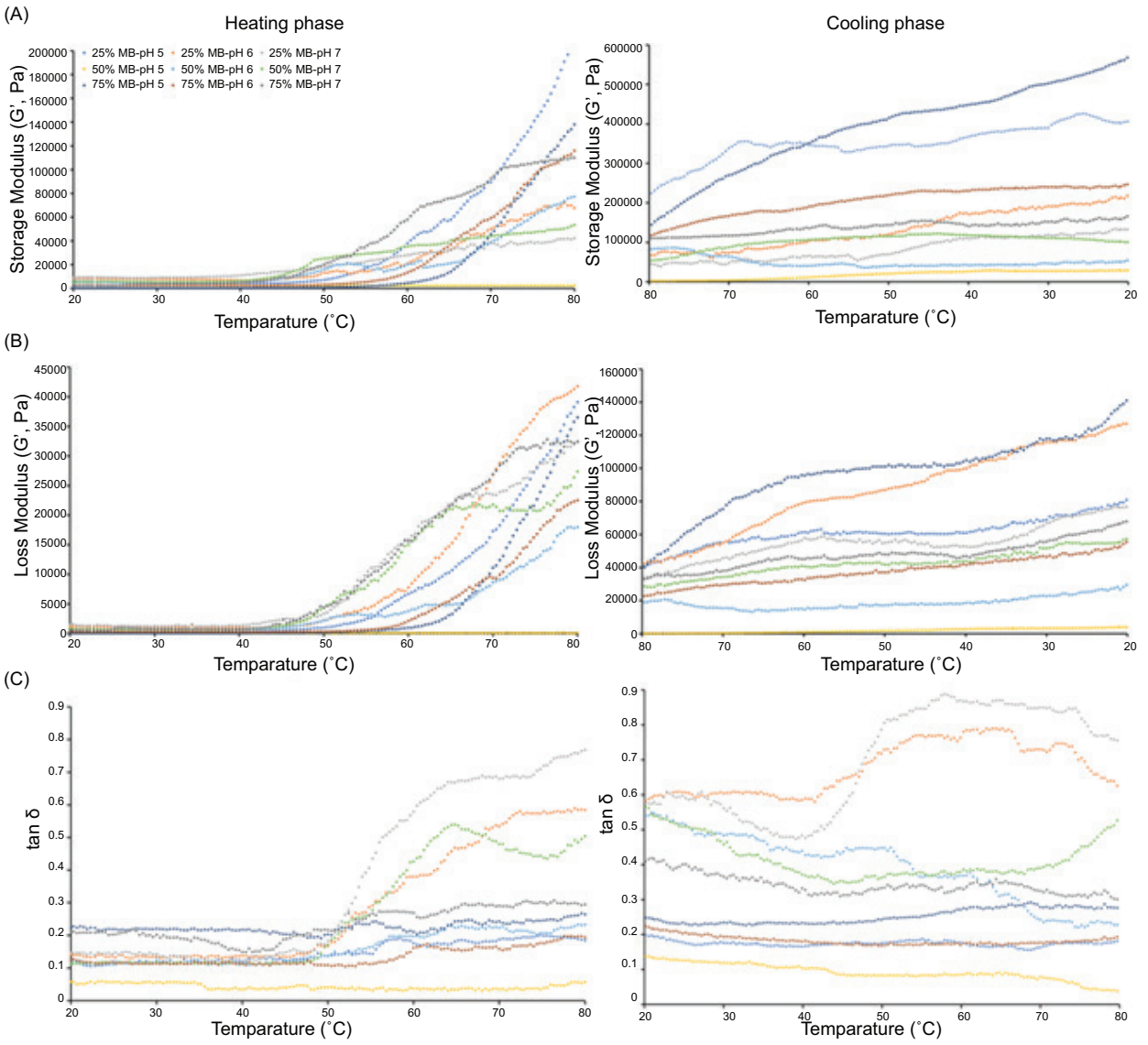

Figure 4. Representative rheograms illustrating (A) energy storage modulus (G'); (B) energy loss modulus (G"); and (C) tangent (tan δ) during heating from 20°C to 80°C and subsequent cooling to 20°C at a rate of 2°C/min for MB-GG composites prepared with different mung bean protein isolate concentrations and pH values. Each point represents the average of three runs.

suggest that increasing MB protein isolate concentration beyond an optimal level does not necessarily enhance gel elasticity in mixed protein–polysaccharide systems (Chassenieux and Nicolai, 2024).

The effect of pH on rheological behavior was also evident. At near-neutral pH conditions (pH 6–7), gels generally exhibited lower increases in G' during heating, compared to those formed at pH 5, particularly for formulations with higher MB protein isolate concentrations. This observation indicates that weak acidic conditions favor stronger thermo-induced gelation in the MB-GG system, consistent with enhanced protein–polysaccharide interactions under such conditions (Malkin and Derkach, 2024). Under these conditions, reduced electrostatic repulsion and improved associative interactions between MB protein and GG potentially promoted more effective network formation during heating, resulting in a stronger viscoelastic response. This behavior may also be attributed to protein aggregation occurring near the isoelectric point of MB protein (approximate pH 4.5–5.0), where reduced net charge minimizes electrostatic repulsion between protein molecules. This promotes closer molecular association and facilitates the formation of a more interconnected network during heating, thereby enhancing thermo-induced gelation.

Table 4. Storage modulus (G') and loss modulus (G") of mung bean protein isolate–low-acyl gellan gum (MB-GG) composites prepared with different MB protein isolate concentrations and pH values before heating (20°C), after heating (80°C), and after cooling to 20°C.

MB (% w/w)	pH	Loss modulus (G", Pa)					
		Heating		Cooling	Heating		Cooling
		20°C	80°C	20°C	20°C	80°C	20°C
25	5	6,080 ± 8.16^{b}	215,000 ± 571.48^{a}	406,000 ± 512.46^{b}	687 ± 2.86^{c}	39,625 ± 82.92^{a}	75,400 ± 91.64^{c}
	6	8,475 ± 12.25^{a}	68,075 ± 120.73^{f}	218,000 ± 316.50^{d}	1,190 ± 8.16^{b}	41,975 ± 63.71^{a}	123,000 ± 124.72^{b}
	7	9,115 ± 69.40^{a}	43,150 ± 107.83^{h}	133,000 ± 200.21^{f}	1,540 ± 17.48^{a}	32,725 ± 71.36^{b}	74,200 ± 62.36^{c}
50	5	2,775 ± 12.25^{e}	2,440 ± 16.99^{g}	29,100 ± 164.97^{h}	180 ± 7.96^{f}	101 ± 3.02^{e}	4,000 ± 40.82^{f}
	6	4,965 ± 62.56^{d}	78,625 ± 80.53^{e}	54,600 ± 149.44^{g}	742 ± 14.51^{c}	18,300 ± 94.39^{d}	29,500 ± 81.65^{e}
	7	5,590 ± 91.66^{c}	54,200 ± 124.22^{g}	108,000 ± 116.49^{e}	786 ± 26.53^{c}	27,500 ± 87.64^{c}	55,500 ± 82.48^{d}
75	5	241 ± 7.75^{f}	139,500 ± 127.21^{b}	568,000 ± 147.40^{a}	68 ± 0.53^{f}	37,775 ± 123.85^{a}	141,000 ± 62.36^{a}
	6	2,760 ± 40.84^{e}	115,750 ± 141.21^{c}	247,000 ± 168.49^{c}	359 ± 7.76^{e}	22,525 ± 94.29^{d}	55,300 ± 40.82^{e}
	7	2,635 ± 24.08^{e}	95,075 ± 93.63^{d}	166,000 ± 123.61^{e}	556 ± 8.22^{d}	32,575 ± 63.96^{b}	67,900 ± 62.36^{c}

Notes: Values are expressed as mean ± SD (n = 3).
Different superscript alphabets within the same column indicate significant differences among formulations according to Duncan's multiple range test ($P < 0.05$). MB: mung bean.

Overall, the rheological results demonstrate that both MB protein isolate concentration and pH strongly influence the viscoelastic properties and thermal stability of MB-GG gels. The superior elastic behavior observed for gels containing 25% MB protein isolate, especially under acidic conditions, corroborates TPA (Section 3.4) and microstructural observations (Section 3.5), highlighting the critical role of appropriate protein–polysaccharide interactions in the formation of mechanically robust gel networks (Chassenieux and Nicolai, 2024). Comparable trends are reported in other protein–polysaccharide systems, such as canola and sesame protein coacervates with Tragacanth gum, where pH and protein-to-polysaccharide ratio significantly influenced viscoelastic properties and gel strength. These studies demonstrated that balanced electrostatic interactions promote elastic-dominant behavior, whereas deviations from optimal conditions result in weaker and more dissipative structures (Ghorbani *et al.*, 2025).

The tan δ profiles further supported the viscoelastic behavior of MB-GG gels (Figure 4C). In all samples, tan δ remained below 1 throughout heating and cooling, confirming the predominance of elastic behavior over viscous behavior. Formulations containing 25% MB protein isolate generally exhibited lower tan δ values, indicating a stronger and more stable gel network, whereas those with higher MB protein isolate concentrations showed higher tan δ values, particularly during heating, reflecting a greater viscous contribution and weaker network organization. During cooling, tan δ tended to stabilize or decrease slightly, suggesting structural reinforcement of gel matrix. These rheological differences indicate that the viscoelastic behavior of MB-GG systems was governed not only by total solids content but also by the balance between protein aggregation, GG continuity, and intermolecular association efficiency during thermal gelation.

Zeta potential

The zeta potential values of MB-GG composites prepared at different MB protein isolate concentrations and pH levels are presented in Figure 5. All formulations exhibited negative zeta potential values, indicating that the surface charge of the composite systems was dominated by negatively charged groups, primarily originating from GG carboxylate moieties (Abdl Aali *et al.*, 2024). GG carries negatively charged carboxyl groups under the studied pH conditions, whereas MB protein exhibits pH-dependent surface charge with an isoelectric point around pH 4.5–5.0. At pH values above this point, protein also carries a net negative charge, which may lead to electrostatic repulsion between two biopolymers.

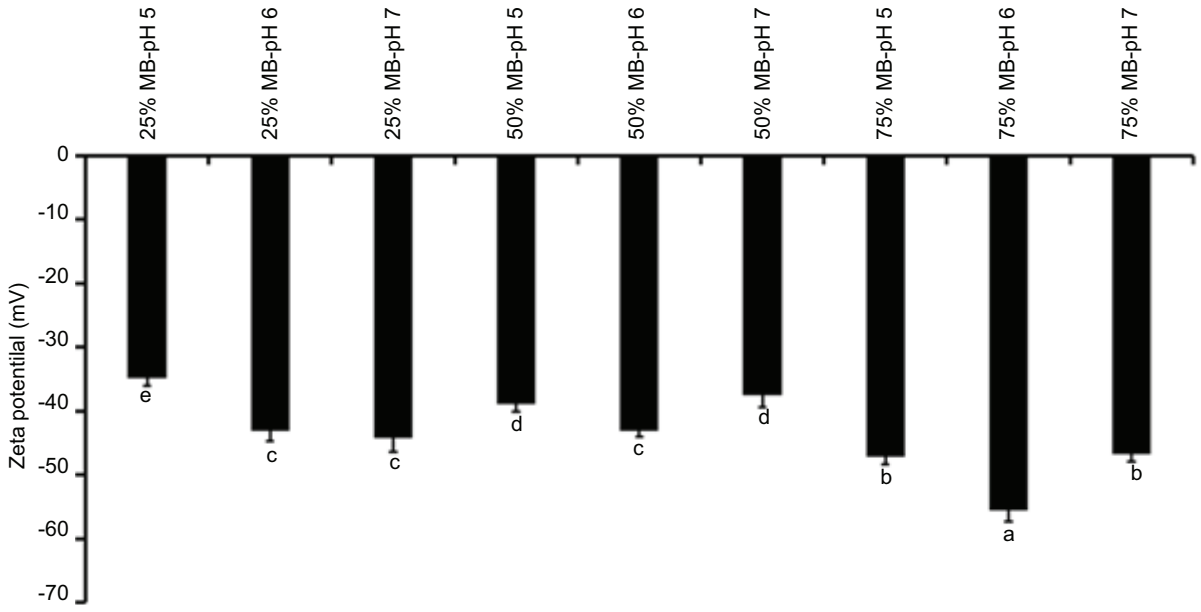

Figure 5. Zeta potential of MB-GG composites prepared with different mung bean protein isolate concentrations and pH values. Different superscript alphabets above the bars indicate significant differences among samples ($P < 0.05$).

For a formulation containing 25% MB protein isolate, the magnitude of negative zeta potential increased with increasing pH, becoming more negative at pH 6 and 7 than at pH 5. A similar trend was observed for the formulation containing 50% MB protein isolate, although the absolute zeta potential values were slightly less negative than those of the 25% system at comparable pH levels. These results suggest that increasing pH enhances the dissociation of acidic groups and increases the net negative surface charge of protein–polysaccharide complexes (Gentile, 2020). Interestingly, the zeta potential did not always become more negative at higher pH (e.g., pH 7, compared to pH 6). This behavior may be attributed to structural rearrangements and charge screening effects within the protein–polysaccharide complexes. At higher pH, increased dissociation of charged groups may enhance intramolecular and intermolecular interactions, leading to partial shielding of surface charges or formation of more compact structures, thereby reducing the apparent zeta potential.

In contrast, the formulation containing 75% MB protein isolate exhibited the most negative zeta potential values among all samples, particularly at pH 6, indicating a substantial increase in surface charge density at higher MB protein isolate concentrations. The significantly more negative zeta potential observed under these conditions suggests enhanced electrostatic repulsion between composite particles, which may influence aggregation behavior and network formation (Abdl Aali *et al.*, 2024; Liu *et al.*, 2025).

The observed variations in zeta potential as a function of pH and MB protein isolate concentration provide direct evidence of pH-dependent electrostatic interactions in the MB-GG system. Conditions associated with intermediate absolute zeta potential values, such as the formulation containing 25% MB protein isolate at pH 5, are indicative of reduced electrostatic repulsion and are favorable for protein–polysaccharide association and network formation (Akpo *et al.*, 2024). This behavior is consistent with the structural and rheological results discussed in Sections 3.5 and 3.6, supporting the role of electrostatic interactions in governing complex coacervation and gel stability (Gentile, 2020; Zheng *et al.*, 2024).

Fourier transform infrared spectroscopy

The FTIR spectra of MB-GG composites prepared at different MB protein isolate concentrations and pH conditions are shown in Figure 6. The spectrum of MB protein isolate exhibited characteristic absorption bands, including a broad O–H and N–H stretching band at 3,200–3400 cm^{-1}, an amide I band centered around 1,650 cm^{-1}, and an amide II band near 1,540 cm^{-1}, which are associated with protein secondary structural features (Huang *et al.*, 2022).

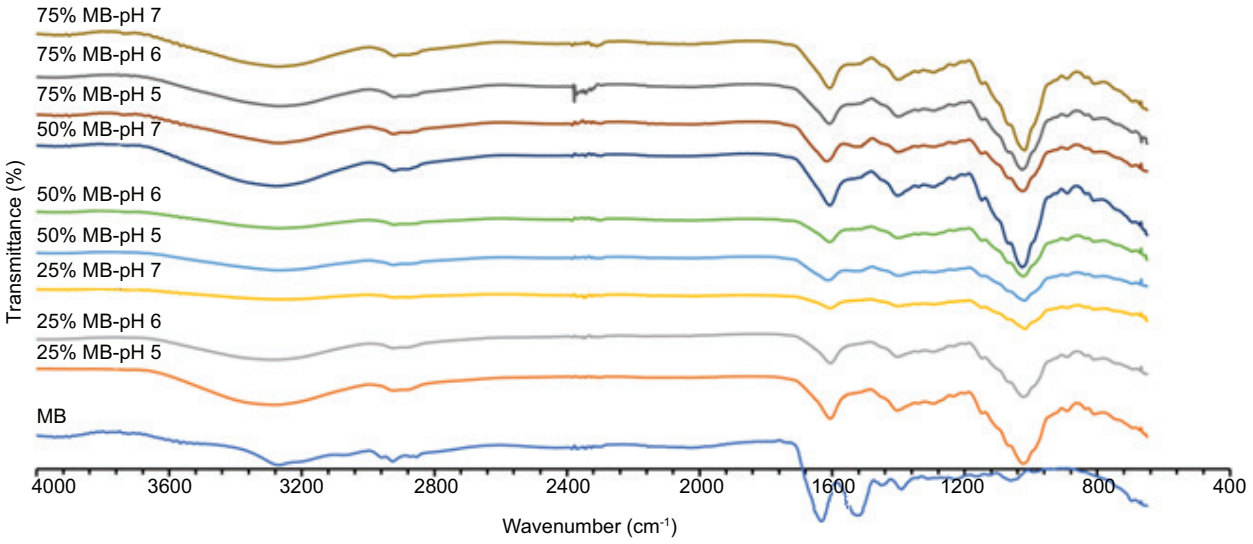

Figure 6. FTIR spectra of MB-GG composites prepared with different mung bean protein isolate concentrations and pH values.

Noticeable changes in the FTIR spectra were observed on incorporation of GG. These included shifts and intensity variations in amide I and amide II bands as well as the appearance of absorption bands in the 1,000–1,150 cm^{-1} region, corresponding to C–O–C and C–O stretching vibrations characteristic of polysaccharides (Binsi *et al.*, 2017; Siaghi *et al.*, 2026). Such spectral modifications indicate the occurrence of intermolecular interactions between MB protein isolate and GG in composite gels.

The observed shifts in the amide I region suggest alterations in protein secondary structure arising from non-covalent interactions, primarily electrostatic attraction between positively charged amino groups of protein and negatively charged carboxylate groups of GG. In addition, changes in the 3,200–3,400 cm^{-1} region (Su *et al.*, 2025), particularly under acidic conditions (pH 5), imply the involvement of hydrogen bonding in stabilizing the protein–polysaccharide network. The magnitude of these spectral changes was more pronounced at lower pH values and tended to decrease with increasing pH, consistent with stronger electrostatic interactions under conditions further from the protein isoelectric point (Sun *et al.*, 2025).

Furthermore, composites prepared with higher MB protein isolate concentrations (50% and 75%) generally exhibited more evident spectral changes than those containing 25% MB protein isolate, suggesting an increased probability of protein–polysaccharide interactions at elevated protein concentrations. FTIR-based evidence of non-covalent interactions between proteins and polysaccharides is reported in similar protein–carbohydrate systems (Pomsang *et al.*, 2024). Comparable pH- and concentration-dependent interaction behaviors are reported in protein–polysaccharide coacervate systems, highlighting the critical roles of formulation parameters in regulating molecular interactions and gel structure (Bhattarai *et al.*, 2026; Dakhili *et al.*, 2026).

Conclusions

This study demonstrates that both MB protein isolate concentration and pH are the key factors governing gel formation, structural organization, and physical properties of protein–polysaccharide mixed gel systems. All formulations exhibited gel-like behavior, as evidenced by consistently higher storage modulus than loss modulus; however, the formulation containing 25% MB protein isolate, particularly at pH 6, produced the strongest, most continuous, and stable gel network. This behavior highlights the dominant role of GG as the primary structural framework within the composite system. Increasing the MB protein isolate concentration to 50% and 75% did not enhance gel strength and instead led to a deterioration of mechanical properties. This effect is attributed to protein–polysaccharide complex coacervation, which limits the effective participation of GG in forming a continuous gel superstructure. FTIR analysis further supported the presence of non-covalent interactions, including electrostatic interactions and hydrogen bonding, with the most pronounced spectral changes observed under acidic conditions. These results indicate that pH primarily modulated the electrostatic environment of the system, while protein concentration

governed the balance between protein aggregation and GG continuity, together determining network organization and the resulting functional properties of gels. In terms of macroscopic quality attributes, increasing MB protein isolate concentration enhanced sample brightness and yellowness, whereas increasing pH shifted the color toward a greener tone and reduced the WHC of gels. Collectively, these results demonstrate that balanced protein–GG interactions, rather than protein enrichment alone, govern gel functionality, structural integrity, and mechanical performance of MB-GG. Overall, these findings provide practical guidance for formulation design in structured plant-based foods and may also serve as a useful framework for understanding structure–function relationships in other plant protein–hydrocolloid systems.

Data Availability Statement

All data necessary to support the conclusions of this research are contained in the article. Raw data files are available from the corresponding author upon reasonable request.

Acknowledgments

The authors would like to thank School of Food Industry, King Mongkut's Institute of Technology Ladkrabang (KMITL), and Department of Industrial Chemistry, Faculty of Applied Science and Food and Agro-Industry Research Center, King Mongkut's University of Technology North Bangkok (KMUTNB), for their contributions and providing all necessary facilities to conduct this research work. Mandatory Disclosure on Use of Artificial Intelligence

Artificial intelligence (AI) tools were used only for language refinement and grammatical editing during manuscript preparation. The authors reviewed and verified all content and take full responsibility for the accuracy and integrity of the manuscript.

Author Contributions

Praewa Lergchinnaboot: writing—review & editing and writing of original draft, methodology, investigation, and formal analysis. Nachomkamon Saengsuk: supervision, resources, writing—review & editing and writing of original draft, project administration, funding acquisition, funding acquisition, visualization, software, methodology, investigation, data curation, conceptualization, and formal analysis. Chanikan Sonklin: methodology and conceptualization. Putthapong Phumsombat: writing—original draft, methodology, formal analysis, investigation, and software.

Conflicts of Interest

The authors declared no conflict of interest.

Funding

This research received no external funding.

References

Abdl, A, Karim, R.A. and Al-Sahlany, S.T.G. 2024. Gellan gum as a unique microbial polysaccharide: its characteristics, synthesis, and current application trends. Gels 10(3): 183. https://doi.org/10.3390/gels10030183

Ahmad, M., Qureshi, S., Akbar, M.H., Siddiqui, S.A., Gani, A., Mushtaq, M., Hassan, I. and Dhull, S.B. 2022. Plant-based meat alternatives: compositional analysis, current development and challenges. Applied Food Research 2(2): 100154. https://doi.org/10.1016/j.afres.2022.100154

Akpo, E., Colin, C., Perrin, A., Cambedouzou, J. and Cornu, D. 2024. Encapsulation of active substances in natural polymer coatings. Materials 17(11): 2774. https://doi.org/10.3390/ma17112774

Alavi, F., Emam-Djomeh, Z. Yarmand, M.S., Salami, M., Salamia, M., Momena, S. and Moosavi-Movahedic, A.A. 2018. Cold gelation of curcumin loaded whey protein aggregates mixed with k-carrageenan: impact of gel microstructure on the gastrointestinal fate of curcumin. Food Hydrocolloids 85: 267–280. https://doi.org/10.1016/j.foodhyd.2018.07.012

Babaei, J., Khodaiyan, F. and Mohammadian, M. 2019. Effects of enriching with gellan gum on the structural, functional, and degradation properties of egg white heat-induced hydrogels. International Journal of Biological Macromolecules 128: 94–100. https://doi.org/10.1016/j.ijbiomac.2019.01.116

Badjona, A., Bradshaw, R., Millman, C., Howarth, M. and Dubey, B. 2024. Optimization of ultrasound-assisted extraction of faba bean protein isolate: structural, functional, and thermal properties. Part 2/2. Ultrasonics Sonochemistry 110: 107030. https://doi.org/10.1016/j.ultsonch.2024.107030

Bhattarai, S., Katekhong, W., Tan, C., Klinkesorn, U. and Peanparkdee, M. 2025. Development of red rice germ extract-loaded microcapsules by complex coacervation using alternative proteins and polysaccharide as wall materials. Journal of Food Engineering 402: 112698. https://doi.org/10.1016/j.jfoodeng.2025.112698

Binsi, P.K., Nayak, N., Sarkar, P.C., Joshy, C.G., Ninan, G. and Ravishankar, C.N. 2017. Gelation and thermal characteristics of microwave extracted fish gelatin–natural gum composite gels.

Journal of Food Science and Technology 54(2): 518–530. https://doi.org/10.1007/s13197-017-2496-9

Chassenieux, C. and Nicolai, T. 2024. Mechanical properties and microstructure of (Emul) gels formed by mixtures of proteins and polysaccharides. Current Opinion in Colloid & Interface Science 70: 101781. https://doi.org/10.1016/j.cocis.2023.101781

Dakhili, S., Yekta, R., Bayanati, M., Sanej, K.D., Mohammadifar, M.A., Nayebzadeh, K. and Shojaee-Aliabadi S. 2026 Optimized complex coacervation and tailored cross-linking of faba protein–xanthan gum complexes for enhanced structural stability and emulsifying performance [In Eng]. Food Chemistry 500: 147537. https://doi.org/10.1016/j.foodchem.2025.147537

Demircan, E., Aydar, E.F., Mertdinc Mertdinç, Z., Kasapoglu Kasapoğlu, K.N. and Ozcelik Özçelik B. 2023. 3D printable vegan plant-based meat analogue: fortification with three different mushrooms, investigation of printability, and characterization. Food Research International 173(1): 113259. https://doi.org/10.1016/j.foodres.2023.113259

Gentile, L. 2020. Protein–polysaccharide interactions and aggregates in food formulations. Current Opinion in Colloid & Interface Science 48: 18–27. https://doi.org/10.1016/j.cocis.2020.03.002

Ghorbani, A., Rafe, A., Hesarinejad, M.A. and Lorenzo, J.M. 2025. Effect of pH and protein to polysaccharide ratio on coacervation of sesame protein isolate-Tragacanth gum: structure-rheology function. International Journal of Biological Macromolecules 311: 143911. https://doi.org/10.1016/j.ijbiomac.2025.143911

Ha Sim, J., Moon, S., Kim, J.H., Lee, C. and Yu, D. 2025. Influence of plant-based gel binders and Song- Hwa mushroom crosslinking on functional properties and consumer perception of vegan mushroom sausage analogues. Food Chemistry 481: 143806. https://doi.org/10.1016/j.foodchem.2025.143806

Hu, X., Ju, Q., Koo, C. and McClements, D. 2024. Influence of complex coacervation on the structure and texture of plant-based protein-polysaccharide composites. Food Hydrocolloids 147: 109333. https://doi.org/10.1016/j.foodhyd.2023.109333

Huang, Z., Yang, X., Liang, S., Chen, L., Dong, L., Rahaman, A., He, S., Shen, Y. and Su, D. 2022. Polysaccharides improved the viscoelasticity, microstructure, and physical stability of ovalbumin-ferulic acid complex stabilized emulsion. International Journal of Biological Macromolecules 211: 150–158. https://doi.org/10.1016/j.ijbiomac.2022.05.078

Kamer, D.D.A., Gumus, T., Palabiyik, I., Demirci, A.S. and Oksuz, O. 2022. The fermentation-based production of gellan from rice bran and the evaluation of various qualitative properties of gum. International Journal of Biological Macromolecules 207: 841–849. https://doi.org/10.1016/j.ijbiomac.2022.03.168

Li, S., Luo, M., Hu, X., Yan, W., Ryu, J. and McClements, D.J. 2025. Creation of novel animal protein substitutes with potato protein and gellan gum: control of food texture, color, and shape. Food Hydrocolloids 158: 110510. https://doi.org/10.1016/j.foodhyd.2024.110510

Liu, L., Zhang, D., Xiaoxiao, S., Guo, M., Wang, Z., Geng, F., Zhou, X. and Nie, S. 2022 Compound hydrogels derived from gelatin and gellan gum regulates the release of anthocyanins in simulated digestion. Food Hydrocolloids 127: 107487. https://doi.org/10.1016/j.foodhyd.2022.107487

Liu, Y., Liu, Y., Zhong, M., Tuly, J.A., Dong, W., Ren, X. and Ma, H. 2025. Protein–polysaccharide complexes for O/W emulsions: structural engineering and their relevance to food stability and safety. Comprehensive Reviews in Food Science and Food Safety 24(5): e70289. https://doi.org/10.1111/1541-4337.70289

Malkin, A.Y. and Derkach, S.R. 2024. Gelation of polymer solutions as a rheological phenomenon (mechanisms and kinetics). Current Opinion in Colloid & Interface Science 73: 101844. https://doi.org/10.1016/j.cocis.2024.101844

Malkin, A.Y., Derkach, S.R. and Kulichikhin, V.G. 2023. Rheology of gels and yielding liquids. Gels 9(9): 715. https://doi.org/10.3390/gels9090715

Moghadam, A., Ghorbani-Hasan Saraei, A., Rafe, A., Fazeli, F. and Shahidi, S.-A. 2025. Improving the functional properties of canola protein isolate through electrostatic coacervation with soluble fraction of Tragacanth gum. International Journal of Biological Macromolecules 330(2): 148103. https://doi.org/10.1016/j.ijbiomac.2025.148103

Namkieat, P., Borompichaichartkul, C., Ayuni, D., Sapwarobol, S.S. and Phumsombat P. 2025. Tapioca-resistant maltodextrin enhances probiotic survival more effectively than commercial prebiotics under simulated gastrointestinal conditions. Food Bioscience 17: 107358. https://doi.org/10.1016/j.fbio.2025.107358

Ozorio, L., Corradi, A.P. and Perrechil, F. 2024. Pea and rice proteins with gellan gum and monovalent salts for the development of plant-based gels for food applications. Applied Food Research 4(2): 100601. https://doi.org/10.1016/j.afres.2024.100601

Palumbo, F.S., Federico, S., Pitarresi, G., Fiorica, C. and Giammona, G. 2020. Gellan gum-based delivery systems of therapeutic agents and cells. Carbohydrate Polymers 229: 115430. https://doi.org/10.1016/j.carbpol.2019.115430

Phumsombat, P., Saengsuk, N., Laohakunjit, N., Selamassakul, O., Sonklin, C. and Srinuan, P. 2025. Influence of cooking methods on physicochemical characteristics and in vitro protein digestibility of restructured pork steak hydrolyzed by bromelain and reformed by κ-carrageenan. Applied Food Research 5(1): 101019. https://doi.org/10.1016/j.afres.2025.101019

Phumsombat, P., Trisakwattana, K., Ittithanaput, N., Viwatanawatanakarn, N. and Borompichaichartkul, C. 2024. Synbiotic and protein-enriched low-fat Sao Hai rice ice cream. Quality Assurance and Safety of Crops & Foods 16(SP1): 14–27. https://doi.org/10.15586/qas.v16iSP1.1453

Pomsang, P., Phumsombat, P. and Borompichaichartkul, C. 2024. Characterisation of chicken breast and soy proteins glycated with konjac glucomannan hydrolysate. International Journal of Food Science and Technology 59(11): 8917–8925. https://doi.org/10.1111/ijfs.17531

Ryu, J. and McClements, D. 2023. Control of plant-based biopolymer composite gel texture: combining potato proteins with different high acyl-low acyl gellan gum ratios. Food Hydrocolloids 149: 109636. https://doi.org/10.1016/j.foodhyd.2023.109636

Saengsuk, N., Barbut, S. and Laohakunjit, N. 2023. Texture modification of easily chewable pork meat batter for masticatory dysfunction people: effects and interactions of bromelain,

κ-carrageenan, and plant protein hydrolysates. International Journal of Food Science & Technology 59: 197–207. https://doi.org/10.1111/ijfs.16794

Saengsuk, N., Laohakunjit, N., Sanporkha, P., Kaisangsri, N., Selamassakul, O., Ratanakhanokchai, K. and Uthairatanakij, A. 2021 Physicochemical characteristics and textural parameters of restructured pork steaks hydrolysed with bromelain. Food Chemistry 361: 130079. https://doi.org/10.1016/j.foodchem.2021.130079

Saengsuk, N., Laohakunjit, N., Sanporkha, P., Kaisangsri, N., Selamassakul, O., Ratanakhanokchai, K., Uthairatanakij, A. and Waeonukul, R. 2022. Comparative physicochemical characteristics and *in vitro* protein digestibility of alginate/calcium salt restructured pork steak hydrolyzed with bromelain and addition of various hydrocolloids (low acyl gellan, low methoxy pectin and κ-carrageenan). Food Chemistry 393: 133315. https://doi.org/10.1016/j.foodchem.2022.133315

Salminen, H., Sachs, M., Schmitt, C. and Weiss, J. 2022. Complex coacervation and precipitation between soluble pea proteins and apple pectin. Food Biophysics 17(3): 460–471. https://doi.org/10.1007/s11483-022-09726-x

Sha, L. and Xiong, Y.L. 2020. Plant protein-based alternatives of reconstructed meat: science, technology, and challenges. Trends in Food Science & Technology 102: 51–61. https://doi.org/10.1016/j.tifs.2020.05.022

Siaghi, M., Nazemi, Z., Janmohammadi, M. and Radmanesh, F. 2026. Effect of Tragacanth gum on physical and mechanical properties of fish collagen sponge for hemostatic dressing applications. Carbohydrate Polymer Technologies and Applications 13: 101095. https://doi.org/10.1016/j.carpta.2026.101095

Sim, H., Jin, S.M., Kim, J.H., Lee, C. and Yu, D. 2025. Influence of plant-based gel binders and Song-Hwa mushroom crosslinking on functional properties and consumer perception of vegan mushroom sausage analogues. Food Chemistry 481: 143806. https://doi.org/10.1016/j.foodchem.2025.143806

Sonklin, C., Saengsuk, N., Wiyaporn, P., Yodlum, P. and Phumsombat, P. 2026. Effect of hydroxypropyl methylcellulose on physicochemical characteristics of high protein jasmine rice coated with rice protein isolate. Food Science and Technology (LWT) 246: Ar. 119297. https://doi.org/10.1016/j.lwt.2026.119297

Su, C-y., Li, D. and Wang, L-j. 2025. From micropores to mechanical strength: fabrication and characterization of edible corn starch-sodium alginate double network hydrogels with Ca2+ cross-linking. Food Chemistry 467: 142276. https://doi.org/10.1016/j.foodchem.2024.142276

Sun, W., Lu, Q., Chen, J., Fan, X., Zhan, S., Yang, W., Huang, T. and Li, F. 2025. Influences of pH on gelling and digestion-fermentation properties of fish gelatin-polysaccharide hydrogels. Foods 14(15): 2631. https://doi.org/10.3390/foods14152631

Tang, D., Dong, Y., Ren, H., Li, L. and He, C. 2014. A review of phytochemistry, metabolite changes, and medicinal uses of the common food mung bean and its sprouts (Vigna radiata). Chemistry Central Journal 8(1): 4. https://doi.org/10.1186/1752-153X-8-4

Tarahi, M., Abdolalizadeh, L. and Hedayati, S. 2024. Mung bean protein isolate: extraction, structure, physicochemical properties, modifications, and food applications. Food Chemistry 444: 138626. https://doi.org/10.1016/j.foodchem.2024.138626

Tripathi, A., Meena, R., Sobhanan, A., Koley, T.K., Meghwal, M. and Giuffrè, A.M. 2024. Influence of ultraviolet-C irradiation treatment on quality and shelf life of mung bean sprouts during storage. Italian Journal of Food Science 36(4): 180. https://doi.org/10.15586/ijfs.v36i4.2619

Wi, G., Bae, J., Kim, H., Cho, Y. and Choi, M.-J. 2020. Evaluation of the physicochemical and structural properties and the sensory characteristics of meat analogues prepared with various non-animal based liquid additives. Foods 9(4): 461. https://doi.org/10.3390/foods9040461

Zheng, J., Meeren, P.V.d. and Sun, W. 2024. New insights into protein–polysaccharide complex coacervation: Dynamics, molecular parameters, and applications. Aggregate 5(1): e449. https://doi.org/10.1002/agt2.449